Zuo *et al. BMC Veterinary Research* (2025) 21:264
https://doi.org/10.1186/s12917-025-04638-7

BMC Veterinary Research

RESEARCH

Antibacterial effects of cinnamaldehyde and hesperitin on resistant *Glaesserella parasuis* by suppressing QseBC two-component system

Jingru Zuo[1], Lin Liao[1], Yujun Gao[1], Junlin Chen[1], Jiang Teng[1], Weihua Zhang[1], Yuhang Wang[1], Yu Sun[1] and Xiaoqiang Liu[1*]

Abstract

Background *Glaesserella parasuis* (*G. parasuis*) is one of the most important porcine pathogens causing Glässer's disease, and QseBC two-component system (TCS) is associated with various behaviors of *G. parasuis*. Our preliminary tests confirmed that plant-derived compounds cinnamaldehyde (CAL) and hesperitin (HES) exhibited promising antimicrobial activity against *G. parasuis*. Here, we further investigate the antimicrobial effects of CAL and HES on *G. parasuis* and the underlying mechanisms.

Results We observed that CAL and HES affected the morphology and physiology of *G. parasuis* based on the biofilm biomass, confocal laser scanning microscope (CLSM) assay, scanning electron microscope (SEM) assay, and conductivity determination as well as intracellular iron level measurement either used alone or in combination. Moreover, CAL and HES can inhibit QseBC TCS of *G. parasuis* by down-regulating the QseBC related genes and quenching the QseC protein based on quantitative reverse transcription polymerase chain reaction (qRT-PCR) and molecular docking and fluorescence quenching assay. In vivo study further evident that CAL and HES exhibited significant antimicrobial and anti-inflammatory activity on *G. parasuis*-infected mice.

Conclusions These findings suggested that CAL and HES can exert antibacterial activity on resistant *G. parasuis* by targeting QseBC, and they may serve as the promising antimicrobial agents for the treatment of *G. parasuis* infection.

Keywords Cinnamaldehyde, Hesperitin, *Glaesserella parasuis*, QseBC, Two-component signaling system

*Correspondence:
Xiaoqiang Liu
liuxiaoqiang142@163.com
[1]College of Veterinary Medicine, Northwest A&F University, Yangling, Shaanxi 712100, PR China

Background

Glaesserella parasuis (*G. parasuis*) is a commensal bacterium in the upper respiratory tract of pigs that has increasingly received attention for causing Glässer's disease, which mainly characterized by fibrinous arthritis, polyserositis, meningitis and some common symptoms of pneumonia [1, 2]. For the last few years, *G. parasuis* has become one of the major causes of nursery morbidity and mortality in swine herds around the world [3, 4], leading to considerable economic losses to swine breeding and food industry [5]. Two-component system (TCS) exists in both prokaryotes and eukaryotes, and it is typically composed with histidine kinase and response regulator. TCS mainly regulate the expression of numerous genes and adaptability of cells to environmental variation [6]. QseBC is a widely distributed TCS in a wide range of bacteria, and it usually plays a pivotal role in the regulation of multiple bacterial behaviors, such as pathogenicity, virulence, biofilm formation and quorum sensing [7]. QseC, a transmembrane protein with histidine kinase activity, becomes activated upon sensing signals from the host and bacteria [8]. Then, it phosphorylates the response regulator QseB, which acts as a transcription factor to regulate the expression of relevant virulence genes. In *G. parasuis*, QseC was associated with biofilm formation, stress response, epinephrine sensing and iron utilization [9]. Therefore, QseBC should be a promising target to develop antimicrobial agents for the treatment of *G. parasuis* infection. Nowadays, the most widely accepted treatment for *G. parasuis* infection is antibiotics, whereas the inevitable side effect of antibiotics is the emergence of multidrug resistant isolates, which has become a major concern for global public health owing to its limited therapeutic options. In response to the antimicrobial resistance, QseBC inhibitors can be timely screened and used as an alternative anti-infective agents.

In recent years, lots of effective and safe natural bioactive products have gained much attention due to their antibacterial and anti-inflammatory properties [10]. Our preliminary tests confirmed that cinnamaldehyde (CAL) and hesperitin (HES) exhibited promising antimicrobial activity against *G. parasuis in vitro* after we screened dozens of natural bioactive products. CAL (3-phenyl-2-propenal) is the most abundant bioactive component of cinnamon oil from some plants of the genus *Cinnamomum*, and it possess anticancer, antifungal, anti-inflammatory and a broad spectrum of antimicrobial properties [11–14]. Meanwhile, CAL is also recognized as a safe material and permitted in food applications by the United States Food and Drug Administration [15]. Additionally, flavonoid compounds have drawn the attention as their antioxidant, anti-inflammatory, anticholesterolemic, antimicrobial, and anti-atherosclerotic activities [16]. HES is a flavonoid existing in citrus fruits, such as orange peel and grapefruit, and it have a wide range of pharmacological actions, including anti-inflammatory, antioxidant, antiviral, and anticancer properties according to earlier research [17–20]. So far, the effectiveness and precise mechanisms of CAL and HES against *G. parasuis* remain to be elucidated, and no reports have addressed the combination of aldehyde and flavonoid compounds on *G. parasuis*. Hence, the current study aimed to investigate the antimicrobial activities and the underlying mechanisms of CAL and HES against *G. parasuis* either used alone or in combination both in vitro and in vivo.

Materials and methods

Bacteria strain, culture conditions, reagents and animals

Four *G. parasuis* strains were kindly presented by China Institute of Veterinary Drug Control (Beijing, China), and finally one *G. parasuis* strain with moderate biofilm-forming ability was finally used in this study. *G. parasuis* was generally grown in Tryptice Soy Broth (TSB) and Tryptice Soy Agar (TSA) (Hopebio Co., Qingdao, China). CAL and HES were purchased from Yuanye Bio-Technology Co., Ltd. (HPLC, purity ≥ 98%, Shanghai, China). They were dissolved in dimethyl sulfoxide (DMSO) and sterilized through a 0.22 μm polytetrafluoroethylene syringe filter, and finally obtained 512 μg/mL stock solution. The twelve antibiotics (ampicillin, ceftazidime, ceftriaxone, ceftizoxime, meropenem, amikacin, kanamycin, tetracycline, doxycycline, tylvalosin, thiamphenicol, florfenicol) used in this study were purchased from Dalian Meilun Biotechnology Ltd (Dalian, China; purity > 98%). The BALB/c mice (6–8 weeks old, female, approximately 20 g) were purchased from Chengdu Dossy Experimental Animals Co., Ltd. (Xi'an, China), and kept for 7 days before the experiments. All animal experiments were approved and carried out according to the guidelines of the Animals Ethics Committee of Northwest A&F University (2021052).

In vitro susceptibility testing

G. parasuis was cultured in TSB with 5% fetal bovine serum (FBS) and 0.0025% nicotinamide adenine dinucleotide (NAD). After overnight incubation at 37 °C, the broth microdilution method was used to determine the minimum inhibitory concentration (MIC) of *G. parasuis* according to CLSI M07-A9 [21]. Currently, there is no agreed method and clinical breakpoints for most antimicrobials available for broth microdilution susceptibility testing of *G. parasuis* in CLSI [22]. According to previous studies in China, the MICs of gamithromycin, tildipirosin and danofloxacin for *G. parasuis* ranged from 0.008 to 128 μg/mL, 0.125–32 μg/mL, and 0.008–128 μg/mL, respectively [23–25]. Quality control strain *Escherichia coli* (*E. coli*) ATCC 25,922 was obtained from China Institute of Veterinary Drugs Control (Beijing, China). TSB broth containing 0.1% DMSO was used as the solvent control to exclude the influence of the solvent. Furthermore, the checkerboard assay was implemented to determine the MICs of pairwise agents, and then calculate the fractional inhibitory concentration index (FICI). The FICI was interpreted as follows: synergistic effect, FICI ≤ 0.5; partial synergistic effect, 0.5 < FICI ≤ 0.75; additive effect, 0.75 < FICI ≤ 1.0; indifferent effect, 1 < FICI ≤ 4.0; antagonism, FICI > 4.0 [26].

Time-kill assay

In order to investigate the antimicrobial effect of the CAL and HES on *G. parasuis*, the time-kill assay was employed. *G. parasuis* strain was incubated at 37 °C for 18 h, and then CAL or HES were inoculated into 0.5 McFarland turbidity standard to obtain final concentrations of 1/8 MIC, 1/4 MIC, 1/2 MIC, MIC and 2 MIC, and incubated at 37 °C for 24 h. The final concentration of DMSO was no more than 0.1% in this test and subsequent tests. The assay was performed in triplicate.

Biofilm biomass assessment

In vitro biofilm formation ability was determined using crystal violet staining as described previously with some modifications [9]. Briefly, *G. parasuis* was incubated for 18 h at 37 °C, and then added 500 μL of 0.5 McFarland standard *G. parasuis* culture and equivalent volume of CAL or HES solution to a 24-well plate to obtain final concentrations of 1/8 MIC, 1/4 MIC, 1/2 MIC, MIC and 2 MIC. The plate was washed with sterile phosphate-buffered saline (PBS) (pH 7.2–7.4) after incubation at 37 °C for 48 h, subsequently fixed with methanol for 30 min, stained with 500 μL of 0.1% crystal violet for 5 min, and washed with PBS again, respectively. After air-drying, 200 μL 33% acetic acid (v/v) was added to dissolve the dye solution, and measure the absorbance at 570 nm. Assays were performed in triplicate.

Effect of CAL and HES on secreted polymeric substances during *G. parasuis* biofilm formation

The effect of CAL and HES on extracellular polysaccharide production of *G. parasuis* was determined according to a previous study with a few modifications [27]. The biofilm culturing, as well as CAL and HES adding methods were the same as aforementioned procedures. Extracellular DNA (eDNA) was extracted using TIANamp Bacteria DNA Kit (Tiangen Biotech Co. Ltd., Beijing, China), then analyzed for UV absorption intensity at 260 nm. The extracellular protein was determined with BCA Protein Assay Kit (Thermo Scientific™, Rockford, IL, USA), and the bovine serum albumin as a standard. Each assay was performed in triplicate.

Conductivity determination

Different concentrations of CAL and HES (1/8 MIC, 1/4 MIC, 1/2 MIC, MIC and 2 MIC) were prepared to evaluate the effects of CAL or HES on membrane permeability of *G. parasuis*, and 0.5 McFarland turbidity standard with 0.1% DMSO and TSB broth were used as the positive control and negative control, respectively. The bacterial suspension was placed in a constant temperature shaker at 37 °C for 16 h, and the timing began from the constant temperature shake. Then the conductivity of the bacterial solution was measured using supernatant conductivity (TCD1, Leici, Shanghai, China). All measurements were performed in triplicate.

Scanning electron microscope (SEM) assay

Damage to membrane permeability and morphology of *G. parasuis* was evaluated with scanning electron microscopy (SEM) as previously described with some modifications [28]. Briefly, *G. parasuis* was incubated as described above with 1/8 MIC, 1/4 MIC, 1/2 MIC and MIC of CAL and HES, respectively. The bacteria suspension and sterile silicon wafers (5 mm × 5 mm) were simultaneously added to a 24-well plate. Subsequently, the samples were gently washed thrice with 0.1 M PBS solution, and added 2.5% glutaraldehyde to fix overnight. Gradual dehydration was performed by exposing the samples to increasing percentages of ethanol twice at 30%, twice at 50%, once at 70%, once at 90%, and twice at 100% for a duration of 10 min each time. Finally, the samples were dried in a critical point dryer using CO_2 and coated with a layer of gold-palladium, and then observed under SEM (Nano SEM-450, FEI Company, Hillsboro, OR, USA).

Live/dead bacteria staining assay

Live/dead bacterial staining assays were carried out using a confocal laser scanning microscope (CLSM, A1+/A1R+, Nikon, Tokyo, Japan) to confirm the antibacterial activities of CAL and HES. All tests were carried out according to the relevant instructions of the Live/dead Bacterial Staining Kit (EX3000, Solarbio, Beijing Solarbio Science & Technology Co., Ltd). The living bacteria were colored green, and the dead bacteria were colored red [29].

Intracellular total and ferrous iron level measurement

G. parasuis was incubated for 18 h at 37 °C, 5 mL of 0.5 McFarland turbidity standard with varying concentrations of CAL (1/4 MIC), HES (1/4 MIC), and combination of CAL and HES (1/8 MIC and 1/8 MIC) was incubated at 37 °C for 18 h. The Total Iron Colorimetric Assay Kit (E-BC-K139-M, Elabscience, USA) and Ferrous Iron Colorimetric Assay Kit (E-BC-K881-M, Elabscience, USA) were used to quantify the content of intracellular total and ferrous iron.

Expression levels of QseBC related genes

The expression levels of QseBC related genes were evaluated by quantitative reverse transcription polymerase chain reaction (qRT-PCR). Briefly, *G. parasuis* was incubated as described above with 1/8 MIC, 1/4 MIC, and 1/2 MIC concentrations of CAL or HES, the untreated bacterial suspension was used as negative control. Total RNA was extracted with Trizol reagents, and quantified using NanoDrop2000 spectrophotometer (Thermo Fisher Scientific, Waltham, MA, USA). Reverse transcription from RNA to cDNA was performed using Takara PrimeScript™ RT Reagent Kit (Takara, Beijing, China). Furthermore, qRT-PCR analysis was conducted utilizing PrimeScript™ One Step RT-PCR Kit (Takara, Dalian, China). 16SrRNA was chosen as housekeeping gene to normalize gene expression data. The PCR amplification protocol was as follows: 95 °C for 5 min, followed by 40 cycles of 95 °C for 30 s, 60 °C for 15 s and 72 °C for 30 s. The primers are listed in Table S1.

Molecular Docking

Molecular docking study was executed to examine the binding pattern between QseBC and CAL and HES. The three-dimensional (3D) structures of QseBC, CAL (PubChem CID: 637511) and HES (PubChem CID: 72281) were obtained through the SWISS-MODEL (https://swissmodel.expasy.org/) and PubChem database, respectively. ERRAT and Ramachandran plot were used to evaluate the rationality of protein model (https://saves.mbi.ucla.edu/). The Autodock Tools 1.5.6 package was used to generate docking input files. Additionally, pymol software was used to visualize the docking results.

Interaction of CAL and HES with QseC protein

In order to further investigate the mechanism and energy transfer of interaction between CAL/HES and QseC protein, the quenching effect of CAL and HES with QseC protein was investigated by fluorescence spectroscopy [30]. Firstly, QseC protein expression was performed in *E. coli* strain BL21 (DE3), and BL21 containing plasmid pET32a-QseC (primers are listed in Table S1) was inoculated in LB broth containing 50 mg/mL of kanamycin. Then, the bacteria solutions were induced with isopropyl-β-d-thiogalactoside (IPTG), lysed by sonication on ice, applied to His Trap column and purified with a Ni^{2+}-column. Finally, the QseC protein was eluted with gradient imidazole solution and verified by Sodium dodecyl sulfate polyacrylamide gel electrophoresis (SDS-PAGE). The purified QseC protein was dissolved with HEPES buffer (pH 7.4), and obtained 100 μg/mL of solution. CAL or HES stock solution was diluted to serial twofold dilutions from 1 μg/mL to 1 mg/mL, and 1.5 mL of different concentrations of CAL/HES and isopyknic QseC were added to a cuvette, respectively. The evenly mixed solution was incubated at room temperature for 10 min, and subsequently scanned on the RF-6000 Spectrofluorophotometer (Shimadzu, Kyoto, Japan) and the fluorescent intensity at 250 nm was determined. The DMSO solution and QseC solution were used as blank controls. Excitation and emission wavelength were 500 nm and 200–700 nm, respectively. Finally, the binding constant (Ka) and number of binding site (n) were calculated according to Stern-Volmer equation, respectively.

$\lg[(F0\text{-}F)/F] = \lg Ka + n \lg[Q]$.

F0 and F were the fluorescence intensity without and with CAL and HES, respectively, and [Q] is the concentration of CAL and HES under each fluorescence intensity, unit is μmol/mL.

Protective effect of CAL and HES on *G. parasuis* infection

After acclimation, the female BALB/c mice were randomly divided into the following 9 groups with 6 mice per group: CAL treatment groups (30 mg/kg, 60 mg/kg and 120 mg/kg), HES treatment groups (30 mg/kg, 60 mg/kg and 120 mg/kg), combination of CAL and HES group (30 mg/kg + 30 mg/kg), infection group and control group. CAL and HES were dissolved with 0.5% Carboxymethylcellulose sodium (CMC-Na) by gavage for 7 days, and infected with 3×10^9 CFU of bacterial suspension 6 h after the last dose. The mice of infection group were infected with 3×10^9 CFU of *G. parasuis* and 0.5% CMC-Na, while the mice of control group only received 0.5% CMC-Na. For survival analysis, the mice were administered intraperitoneally with CAL (60 mg/kg), HES (60 mg/kg), or combination of CAL and HES (30 mg/kg + 30 mg/kg), respectively, and 2 h later, each mice was infected with 6×10^9 CFU of *G. parasuis*. Then, mice were monitored daily for signs of morbidity and death. At 96 h postinfection, the survived mice were euthanized with pentobarbital (100 mg/kg, intraperitoneal injection) according to American Veterinary Medical Association (AVMA) Guidelines for the Euthanasia of Animals (2020), the left lung tissue was fixed with 4% paraformaldehyde, and embedded in paraffin. The 4 μm sections were stained with hematoxylin and eosin (H&E) for histopathological analysis. For lung bacterial load analysis, part of right lung tissue was taken for homogenization and CFU determination. For inflammatory factor detection, qRT-PCR was applied to evaluate the expression levels of TNF-α, IL-1β and IL-6. GADPH was employed as a housekeeping gene. The primers are listed in Table S2.

Statistical analysis

Each study was repeated three times independently. Statistical comparison between groups was analyzed using Student's *t* test or one-way analysis of variance (ANOVA) using SPSS v.13.0, and survival curve was analyzed using

Table 1 MICs of antimicrobial agents against *G. parasuis*

Antibiotics	MIC (μg/mL)	
	G. parasuis	***E. coli* (ATCC 25922)**
Ampicillin	32	1
Ceftazidime	8	1
Ceftriaxone	1	1
Ceftizoxime	1	1
Meropenem	2	0.5
Amikacin	32	1
Kanamycin	4	1
Tetracycline	1	1
Doxycycline	4	0.25
Tylvalosin	32	1
Thiamphenicol	4	1
Florfenicol	4	1

Table 2 FIC index of the combination of CAL and HES with AMP, AMK and TAT against *G. parasuis*

Antimicrobial agents	FIC index	
	CAL	**HES**
Ampicillin	0.531	0.531
Amikacin	0.562	0.531
Tylvalosin	0.531	0.375
CAL		0.375

log-rank test. Significant differences among groups were analyzed by one-way ANOVA, followed by Tukey's HSD post hoc test using SPSS v.13.0. $P < 0.05$ were considered statistically significant.

Results

In vitro susceptibility testing

The MICs of CAL and HES against *G. parasuis* were both 128 μg/mL. MICs of several antibiotics against *G. parasuis* were demonstrated in Table 1. Collectively, these data indicated that *G. parasuis* was resistant to ampicillin (AMP), amikacin (AMK) and tylvalosin (TAT) with MICs were 32 μg/mL. In addition, the effect of CAL or HES in combination with AMP, AMK and TAT against *G. parasuis* was displayed in Table 2. The results revealed that the combination of CAL with AMP, AMK or TAT showed partial synergistic effect with FICI ranging 0.531–0.562. Additionally, the combination of HES with AMP and AMK also showed the partial synergistic effects, while the combination of HES with TAT, and the combination of HES and CAL showed the significant synergistic effect.

Time-kill curves of CAL and HES

The time-kill curves of CAL and HES against *G. parasuis* was shown in Fig. 1. Compared to the OD_{600} value of control, 1/8 MIC, 1/4 MIC, 1/2 MIC and MIC of CAL showed certain inhibitory effects on *G. parasuis* growth in a concentration-dependent manner (Fig. 1A). Although the 1/8 MIC of CAL experienced partial growth inhibition during the first14-h period, and the growth pattern was similar to the control group after 14 h. However, *G. parasuis* exhibited significant inhibition of growth at1/4 MIC and 1/2 MIC of CAL. Moreover, the OD_{600} values of the MIC and 2 MIC groups were almost unchanged, it was further confirmed that CAL could effectively delay the growth of *G. parasuis*. As shown in Fig. 1B, the effects of 1/8 MIC, 1/4 MIC and 1/2 MIC of HES on *G. parasuis* growth during the first 12 h were similar, and the growth curve of the 1/8 MIC group was similar to the control group after 12 h. Similarly, the MIC and 2 MIC of HES groups almost unchanged. Furthermore, there was nearly no difference in growth trends between the combination group and the control group (1/8 MIC of CAL and 1/8 MIC HES), with almost no inhibition (Fig. 1C). The OD_{600} values of these three groups (1/2 MIC of HES + 1/4 MIC of CAL, 1/2 MIC of HES + 1/8 MIC of CAL, 1/2 MIC of CAL + 1/4 MIC of HES) barely changed in 24 h, and the other groups showed different degrees of inhibition.

Effect of CAL and HES on biofilm formation and secreted polymeric substances

The effects of CAL and HES on *G. parasuis* biofilm formation were demonstrated in Fig. 2. The OD_{570} values gradually increased with the incubation time and reached a peak at 48 h, followed by a gradual plateau. The process of *G. parasuis* biofilm formation includes adhesion, formation of microcolonies, maturation and eventual dispersion of the biofilm in order to adjust to environmental changes, and reveals resemblance to "seed dispersal" [31]. As shown in the Fig. 2A-B, the concentration-dependent inhibition of *G. parasuis* biofilm formation was evident in the 1/2 MIC of CAL and HES when compared to the

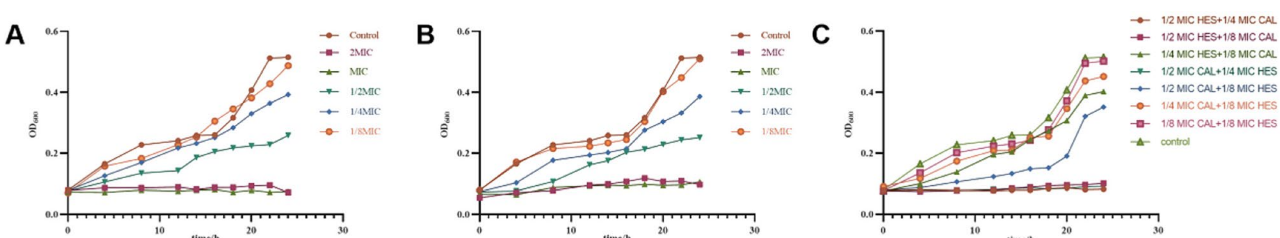

Fig. 1 Time-kill curve of CAL and HES against *G. parasuis*. **A**, CAL; **B**, HES; **C**, combination of CAL and HES

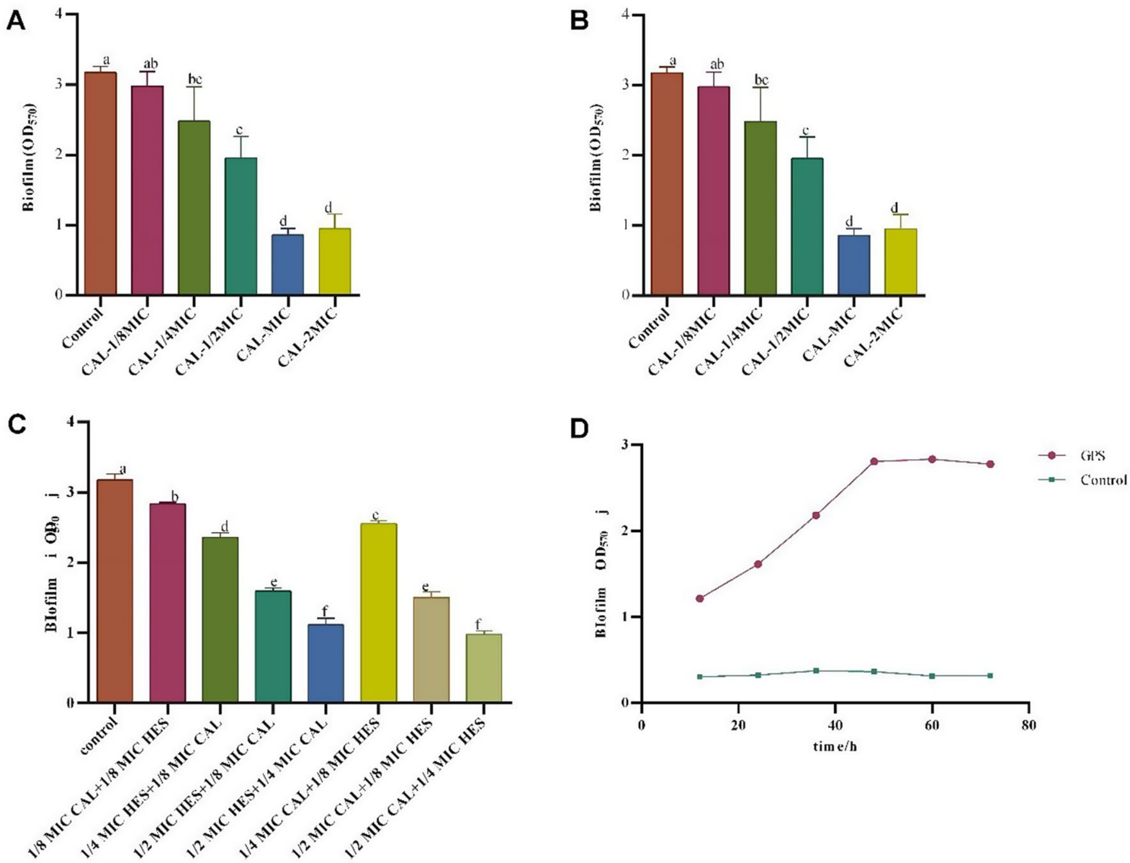

Fig. 2 The effect of CAL and HES on biofilm formation. **A**, CAL; **B**, HES; **C**, combination of CAL and HES; D, biofilm formation at different incubation times. Values denoted by varying lowercase letters signify a notable difference in every treatment ($P < 0.05$), whereas those with identical lowercase letters denote no significant difference ($P > 0.05$)

control OD_{570} values. The inhibition rate of 1/8 – 1/2 MIC of CAL group ranged from 6.18 to 38.47%. Notably, the inhibition ratio of 2 MIC of CAL on *G. parasuis* biofilm formation was 73.0%. The HES exhibited the inhibition rates ranging from 36.17 to 68.64% with a concentration of 1/8 – 1/2 MIC, and the inhibition ratio was 70.32% at 2 MIC. Moreover, the combination of HES and CAL demonstrated an inhibition efficiency varying between 10.73% and 69.10% (Fig. 2C). The combination of 1/8 MIC of CAL and 1/8 MIC HES group showed the minimal inhibitory effect, while the 1/2 MIC of CAL and 1/4 MIC of HES group showed the greatest inhibitory effect.

The secreted polymeric substances have been identified as having a significant inhibitory effect on biofilm formation (Fig. 3A-F). On the one hand, the inhibition rate of CAL, HES and combination group on the extracellular DNA were distributed in the range of 1.12-55.75%, 4.49-77.98% and 5.15-56.84%, respectively. On the other hand, extracellular protein during *G. parasuis* biofilm formation in 1/8 – 2 MIC of CAL, 1/8 – 2 MIC of HES and combination groups were inhibited with percentage ranging from 27.09 to 71.33%, 15.30–66.93%, and 16.90–65.04%, respectively.

Effect of CAL and HES on *G. parasuis* membrane

The extracellular relative electric conductivity can be used to determine whether the membrane permeability of the bacterial cell is altered. The ion efflux from the bacterial body lead to an increase in the conductivity of the bacterial fluid once the bacterial cell membrane was damaged. The electric conductivity of *G. parasuis* treated by 1/8 MIC-2 MIC of CAL and HES were revealed in Fig. 4A and B, and the electric conductivity of 2 MIC of CAL and HES treated *G. parasuis* significantly increased 25.43% and 9.64% compared with the control group, respectively. Besides, the electrical conductivity in the combination of 1/2 MIC of CAL and 1/4 MIC of HES group showed an increase of 15.22% compared with the control group (Fig. 4C).

The antibacterial activities of CAL and HES against *G. parasuis* were further characterized by SEM. As shown in Fig. 5, G. *parasuis* of control group were encapsulated in thick biofilms, which aggregated and adhered to each other to protect the bacteria from adverse external environment, and it is difficult to see the presence of individual bacteria cell. However, the biofilm became thinner, the adhesion ability of bacteria was significantly

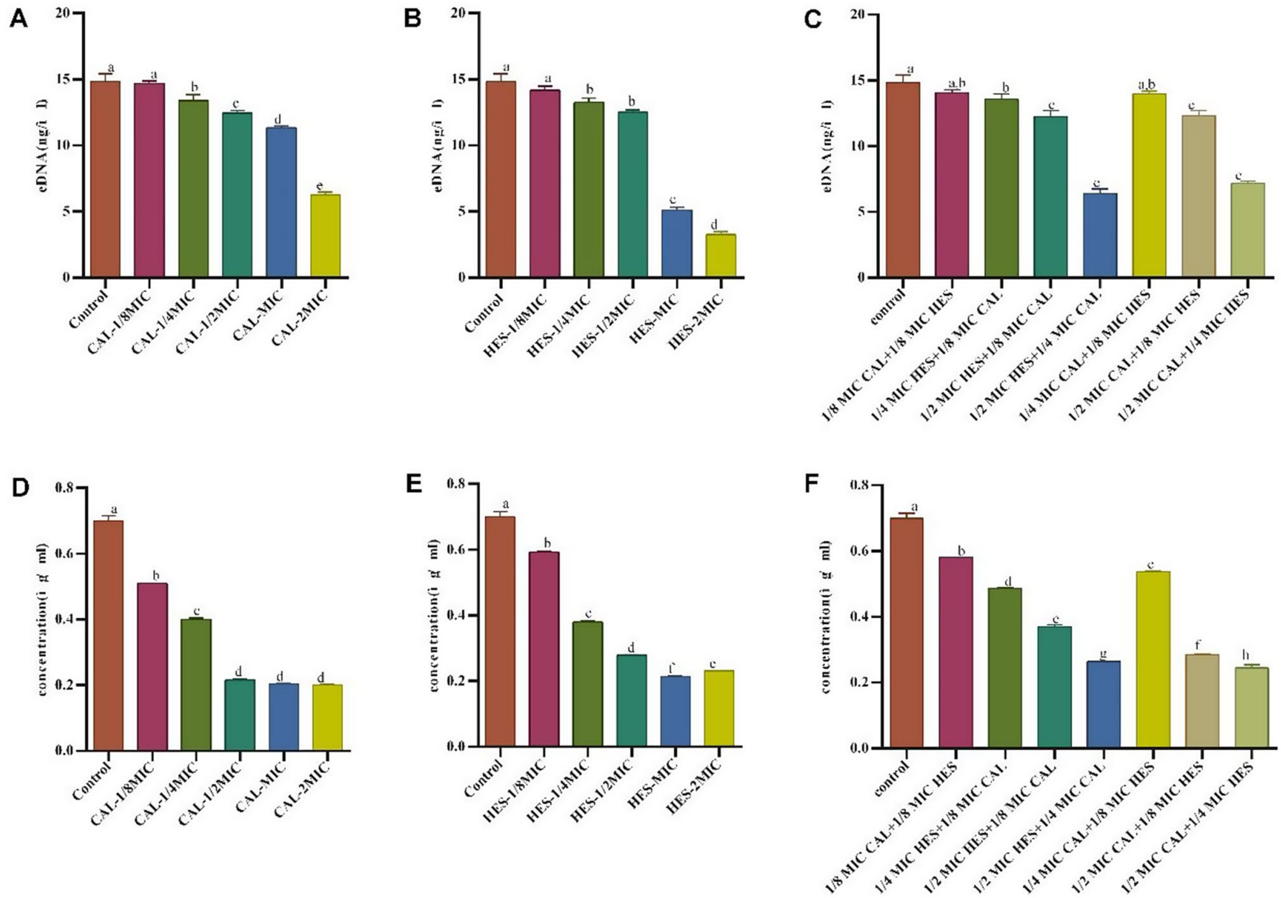

Fig. 3 The effect of CAL and HES on the secreted polymeric substances during *G. parasuis* biofilm formation. **A-C** were the effect of CAL, HES and the combination of CAL and HES on extracellular DNA, respectively; **D-F** were the effect of CAL, HES and the combination of CAL and HES on extracellular protein. Values denoted by varying lowercase letters signify a notable difference in every treatment ($P < 0.05$), whereas those with identical lowercase letters denote no significant difference ($P > 0.05$)

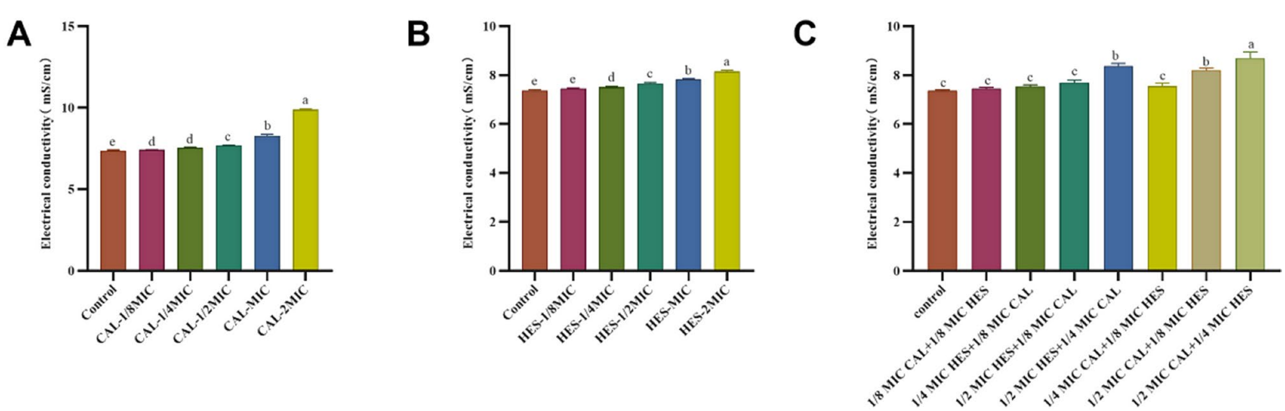

Fig. 4 The effect of CAL (**A**), HES (**B**), combination of CAL and HES (**C**) on electric conductivity with different concentrations. Values denoted by varying lowercase letters signify a notable difference in every treatment ($P < 0.05$), whereas those with identical lowercase letters denote no significant difference ($P > 0.05$)

decreased, and a few short rod-shaped bacteria could be observed on the surface as the *G. parasuis* were treated with1/8 MIC of CAL or HES. Besides, significant biofilm disruption was observed, and the bacteria structure was no longer compact with individuals, the membrane integrity of *G. parasuis* cell was impaired, and the bare *G. parasuis* cells were scattered outside the biofilm in 1/4 MIC of CAL or HES group. In 1/2 MIC of CAL or HES

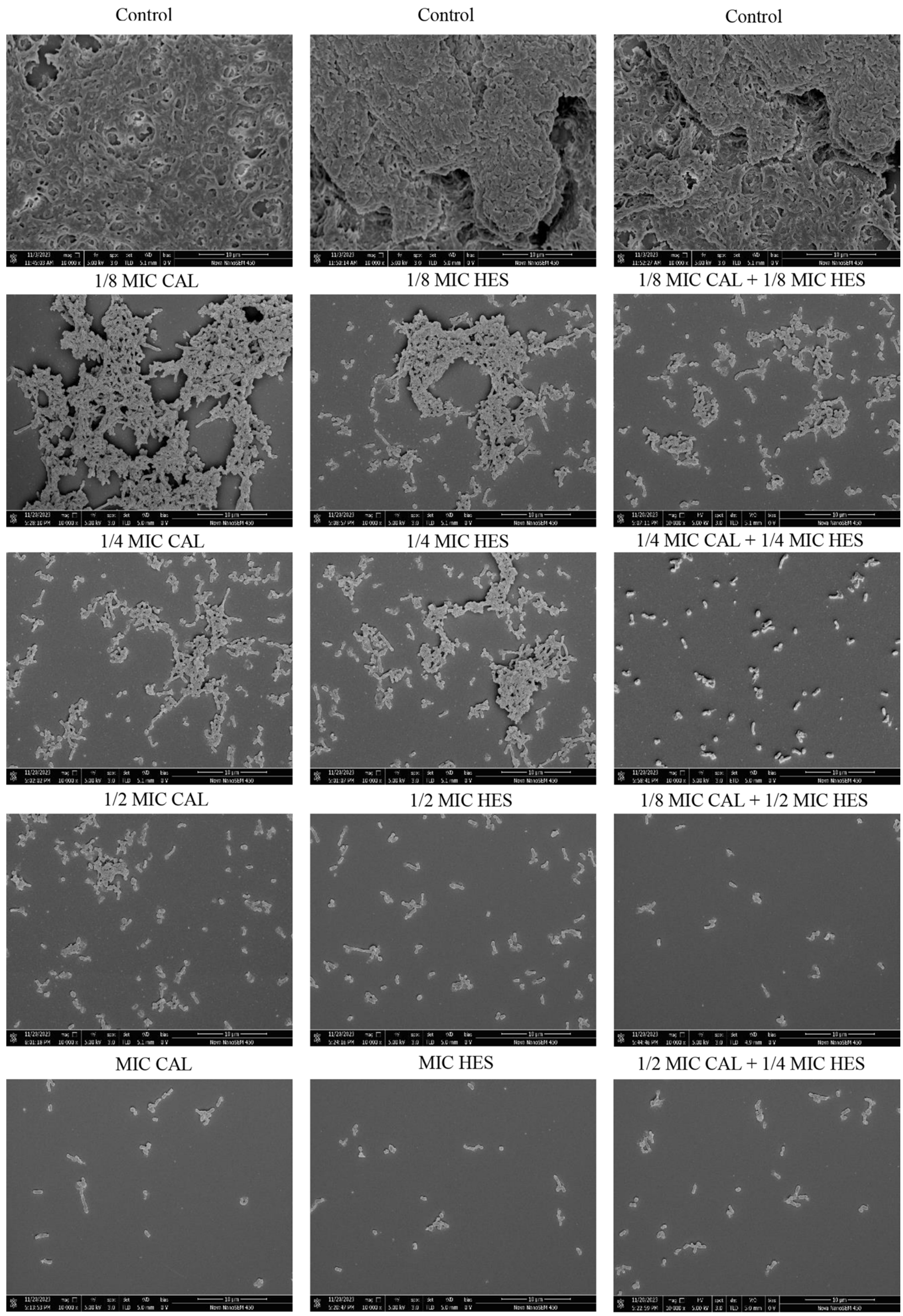

Fig. 5 Morphological changes of *G. parasuis* treat with CAL and HES

groups, only a small amount of biofilms were observed, a large proportion of *G. parasuis* which were exposed to CAL and HES appeared a high degree of malformation and damaging. Furthermore, the effects on the bacterial biofilms were further aggravated after treatment with MIC of CAL and HES, and some bacteria cells completely lost their normal shape and even ruptured, whereas untreated cells showed a regular rod-sharped structure with an intact cell membrane. Overall, the above results further indicated that the CAL and HES had potent antibacterial activities in a concentration-dependent manner. It is noteworthy that the combination of CAL and HES

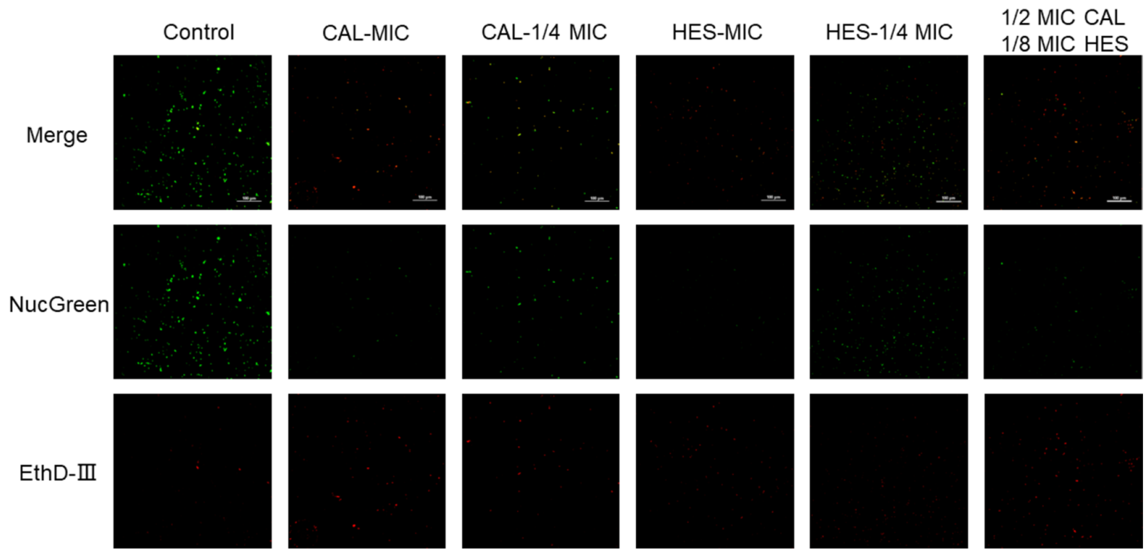

Fig. 6 Live/Dead bacteria staining observation with or without CAL and HES treatment (Fluorescence microscope×100)

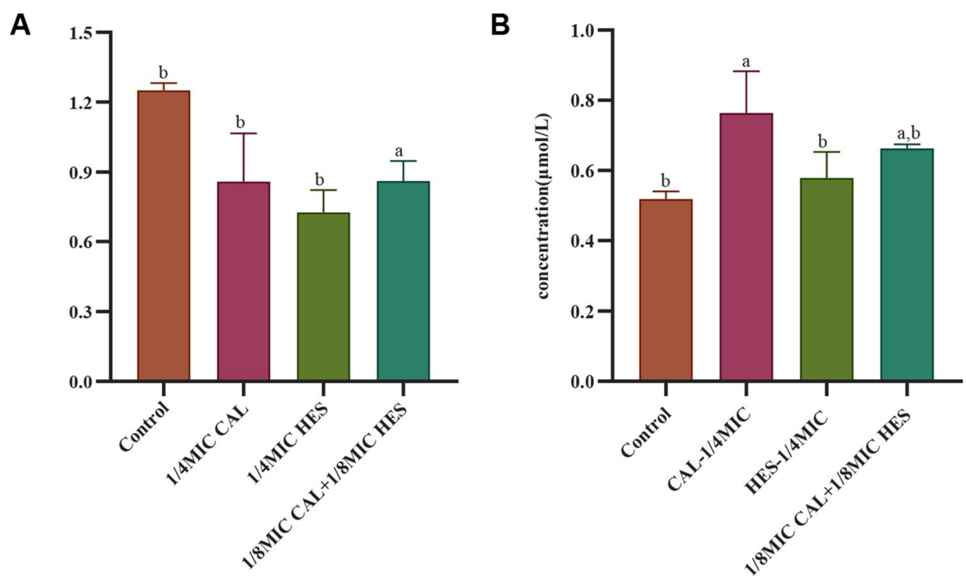

Fig. 7 Effects of CAL and HES on iron utilization in *G. parasuis*. **A**, total iron; **B**, ferrous iron

was more effective than the single use of CAL or HES at the same concentration.

To further investigate the impact of CAL and HES on bacterial membranes, CLSM employing NucGreen and EthD-III dyes was utilized to assess the bacterial cell membrane's integrity [32]. As shown in Fig. 6, the control group was almost exclusively green fluorescent with intact cell membranes, appeared to agglomerate with clumped green fluorescence. Additionally, the cell membrane of bacteria treated with CAL and HES was damaged, which showed different degrees of red fluorescence. When *G. parasuis* subjected to MIC of CAL and HES groups, a significant amount of red fluorescence was observed, while only a small part of green fluorescence appeared sporadically. In combination of CAL and HES, 1/4 MIC of CAL and 1/4 MIC of HES groups, the bacteria exhibited reduced red fluorescence, indicating that either alone or in combination of sub-MIC of CAL and HES caused damage to *G. parasuis* membrane.

Effects of CAL and HES on iron utilization in *G. parasuis*

The absorption of iron primarily happens via two main pathways [33]. Bacteria have the capability to import the ferric and ferrous iron via iron-binding siderophores, while the free ferrous ions could permeate the bacteria's periplasm through porins, eventually being conveyed into the cytoplasm by a series of cytoplasmic proteins. As depicted in Fig. 7, with the treatment of CAL and

HES, there was a reduction in intracellular iron levels, an increase in ferrous iron, and a higher percentage of ferrous iron compared to ferric iron. Obviously, the proportion of ferrous iron decreased from 88.92 to 41.49%, and the proportion of ferric iron increased from 11.08 to 58.51% in CAL group with 1/4 MIC. It implied that both CAL and HES might have influenced bacterial iron transportation by targeting QseBC TCS.

Effect of CAL and HES on the expression of QseBC related genes

qRT-PCR analysis was conducted to assess the effects of CAL and HES on the expression of QseBC related genes, including β-lactam resistance (*oppB*), peptidoglycan biosynthesis (*mraY* and *macB*), biofilm formation (*crp* and *lpxM*), virulence (*cdtA*, *cdtB* and *ompP2*), bacterial chemotaxis (*rbsB*) and bacterial flagellum (*pilW*). Generally, CAL and HES repressed the tested genes by 2- to 14-fold (Fig. 8A-F). Among of them, the expression of *oppB* decreased about 5-fold and 3-fold in 1/2 MIC of CAL and HES groups, respectively, while it decreased 11-fold in the combination of 1/8 MIC of HES and 1/4 MIC of CAL group. Additionally, the expression of *mraY* and *macB* decreased approximately 6-fold and 4-fold in the 1/2 MIC of CAL group, 6-fold and 14-fold in the 1/2 MIC of HES group, 3-fold and 2-fold in the combination of 1/8 MIC of HES and 1/4 MIC of CAL group, respectively. The *crp* and *lpxM* genes were down-regulated 8-fold and 5-fold in the 1/2 MIC of CAL group, 11-fold and 9-fold in the 1/2 MIC of HES group, and 2-fold in the combination of 1/4 MIC of HES and 1/8 MIC of CAL group, respectively. *cdtA* and *cdtB* were down-regulated 13-fold and 12-fold after 1/2 MIC of CAL treatment, 5-fold and 9-fold after the 1/2 MIC of HES treatment, 13-fold and 10-fold after the treatment with the combination of 1/4 MIC of CAL and 1/4 MIC of HES. Moreover, *ompP2* decreased 7-fold and 8-fold in 1/2 MIC of CAL or HES group, and 8-fold in the combination of 1/4 MIC of HES and 1/8 MIC of

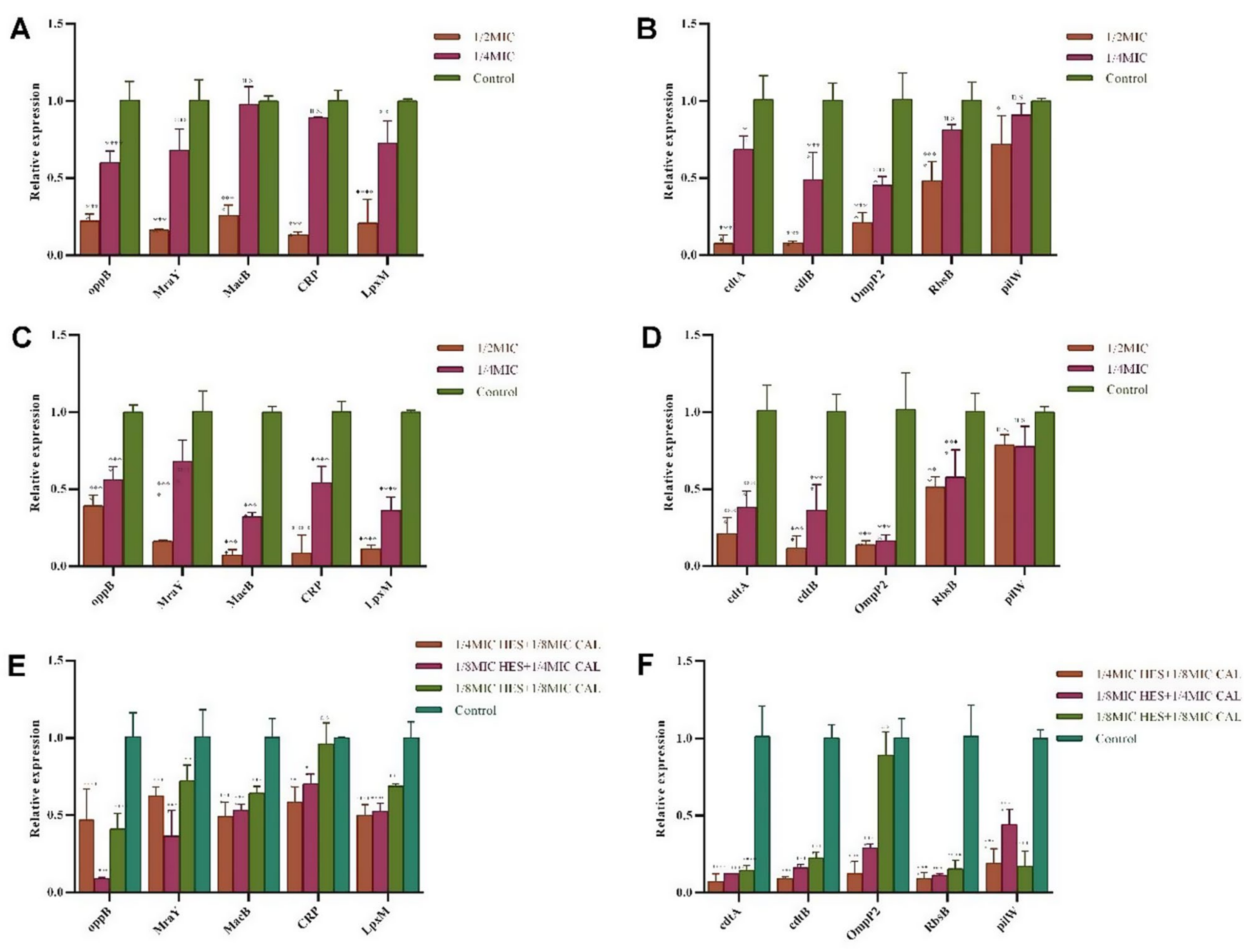

Fig. 8 Effect of CAL and HES on the expression of QseBC related genes. **A-B**, effect of CAL on the expression of related genes. **C-D**, Effect of HES on the expression of related genes; **E-F**, Effect of combination of CAL and HES on the expression of related genes Control groups were set up as 1. Relative transcript levels of *oppB*, *mraY*, *macB*, *crp*, *lpxM*, *cdtA*, *cdtB*, *ompP2*, *rbsB* and *pilW* were represented as mean ± SD of at least three biological replicates. *$P < 0.05$, **$P < 0.01$, ***$P < 0.001$, ****$P < 0.0001$

CAL group, respectively, and the expression level of *rbsB* decreased approximately 2-fold and 11-fold after treatment with 1/2 MIC of CAL and 1/2 MIC of HES, 11-fold in the combination of 1/4 MIC of HES and 1/8 MIC of CAL group. Besides, *pilW* decreased about a 1.3-fold and 5-fold in 1/2 MIC of CAL and HES group, and 5-fold in the combination of 1/4 MIC of HES and 1/8 MIC of CAL group, respectively.

Molecular modeling

As shown in Fig. S1, 3D protein model was constructed using SWISS-MODEL based on known protein model and the amino acid sequence alignment results of QseBC. ERRAT and Ramachandran plot were applied to evaluate the rationality of protein model. Overall, quality factor of QseBC calculated by ERRAT was 95.4 and 93.1, respectively. Residues in most favored regions of QseBC were 92.9% and 90.0%, respectively, implying that protein model is reliable. The binding energies of the docking are −5.73 kcal/mol (QseB-CAL), -5.53 kcal/mol (QseC-HES), -5.95 kcal/mol (QseB-HES) and −5.73 kcal/mol (QseC-HES). LYS-177 of QseB, LYS-417 of QseC and cinnamaldehyde produce hydrogen bonding forces. VAL-148, VAL-141 and ARG-139 produce hydrogen bonding forces with hesperetin; VAL-349, TRP-317 and GLN-385 produce hydrogen bonding forces with hesperetin. The molecular modeling results emphasized that CAL and HES produced interaction forces with QseBC (Fig. S1 C).

Fluorescence quenching spectra of CAL and HES on QseC protein

QseC were successfully expressed in *E. coli* and purified. The result of SDS-PAGE was showed in Fig. S2. As is shown in Fig. 9, QseC has the maximum fluorescence emission at 250 nm, the addition of CAL regularly reduced the fluorescence intensity of QseC at 250 nm (Fig. 9A), it is indicated that there is an interaction between CAL/HES and QseC protein, leading to the changes of certain amino acid residues that produce endogenous fluorescence in QseC, and the fluorescence intensity decreased in a concentration-dependent manner. Moreover, a fitting curve was obtained according to the results to lg[Q] as lg[(F0-F)/F] (Fig. 9E), the Ka were 4.23×10^4 L/moL and 9.28×10^5 L/moL, with the number of binding site (n) were 2.3816 and 2.9489, respectively, suggesting that CAL and HES had powerful abilities to quench the fluorescence of QseC at excitation and emission wavelengths.

Protective effect of CAL and HES on *G. parasuis* infection

An in vivo study was carried out to evaluate the protective effect of CAL and HES on *G. parasuis* infected mice. Figure 10A displayed the representative images of lung tissues and H&E staining of lung sections under the protection of CAL and HES. Control group indicated that lung was light pink with evenly alveolar cavity and elastic state. Inversely, severe bleeding occurred in lung of *G. parasuis* infected mice, and the lung tissue appeared dark red, which had a wide range of inflammatory cell infiltration in H&E staining section. Under the protection of the CAL or HES, lung congestion status was improved, and inflammatory cells infiltration was reduced in a dose dependent manner. Unsurprisingly, the 120 mg/mL of CAL or HES showed obvious protective effect, while the combination of CAL and HES (30 mg/kg + 30 mg/kg) has a better protective effect than high dose of single use of CAL or HES.

Furthermore, to examine the effect of CAL and HES on the survival rate of *G. parasuis* infected mice, CAL, HES, or the combination of CAL and HES were administered intraperitoneally 2 h prior to *G. parasuis* injection. As shown in Fig. 10B. All mice in the infected model group died within 20 h, and the survival rate of mice increased to 16.7% as the infected mice were treated with 60 mg/kg of CAL or HES. It is noteworthy that the survival rate of infected mice reached to 33.3% after treatment with the combination of CAL and HES (30 mg/kg + 30 mg/kg). Additionally, the lung bacterial load were showed in Fig. 10C. The bacterial load decreased from 9×10^9 CFU (control group) to 1.6×10^5 CFU (CAL, 120 mg/kg), 1.3×10^5 CFU (HES, 120 mg/kg) and 1.0×10^5 CFU (CAL + HES, 30 mg/kg + 30 mg/kg).

The effects of CAL and HES on the expression of IFN-γ, IL-6 and TNF-α, three important inflammatory factors associated with antimicrobial immunity, were shown in Fig. 10D-F, and Fig. 10G-I, respectively. Generally, the presence of IFN-γ, IL-6 and TNF-α was notably elevated by *G. parasuis* infection, whereas CAL and HES could dramatically reverse these changes. The expression of IFN-γ decreased approximately 5.4-fold, 4.4-fold and 4.1-fold in HES (120 mg/kg), CAL (120 mg/kg) and CAL + HES (30 mg/kg + 30 mg/kg) group, respectively. The expression of IL-6 showed about 5.5-fold decrease in HES (120 mg/kg) group, 5.2-fold in CAL (120 mg/kg) group, and 3.4-fold in CAL + HES (30 mg/kg + 30 mg/kg) group. In addition, the TNF-α were down-regulated 1.9-fold, 5.7-fold and 3.7-fold in HES (120 mg/kg), CAL (120 mg/kg) and CAL + HES (30 mg/kg + 30 mg/kg) group, respectively. These findings indicated that both CAL and HES exhibited marked anti-inflammatory activity against *G. parasuis* infection.

Discussion

G. parasuis is well-known for causing Glässer's disease, and leading to enormous financial losses for the global pig industry. It usually plays a role in causing respiratory illnesses in pigs and exist as a symbiotic bacterium in the nasal passages of healthy pigs [3]. Meanwhile, *G.*

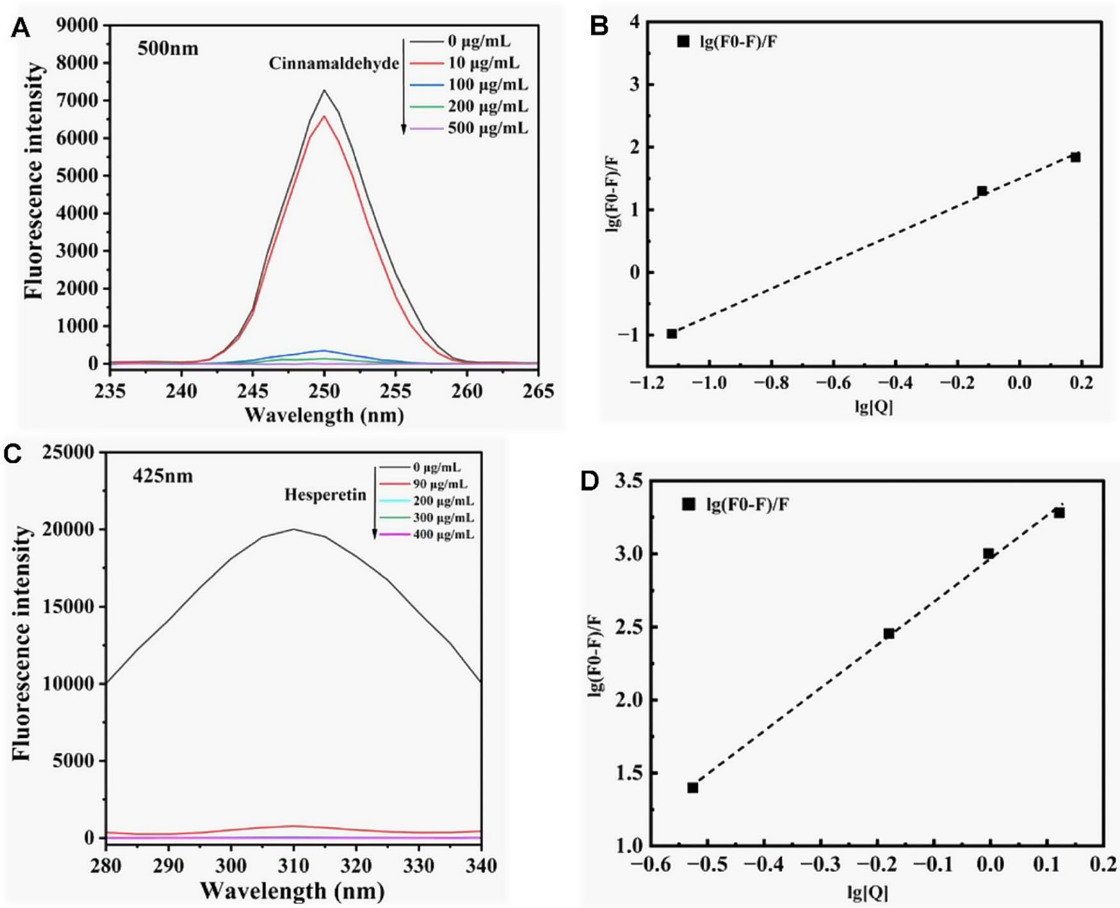

E

	Curve	R^2	*Ka*	n
CAL	Y = 2.3816X + 1.6264	0.9904	4.23×10^4 L/mol	2.3816
HES	Y = 2.9489X + 2.9675	0.9978	9.28×10^5 L/mol	2.3816

Fig. 9 The excitation and absorption spectra range from 235 to 700 nm (**A**, **C**); The fluorescence quenching charts for Stern-Volmer (**B**, **D**) for CAL and HES, respectively

parasuis is frequently co-infected with porcine reproductive and respiratory syndrome virus. It is noteworthy that *G. parasuis* serotype 5 is deemed highly virulent, capable of penetrating the respiratory tract's epithelial barrier, potentially leading to serious lung infections [34]. For the past few years, the antimicrobial resistance of *G. parasuis* continually increased, and even the resistance rate to tetracycline, sulfa and fluoroquinolones exceeded 80% [35, 36]. Therefore, it is necessary to develop alternative antimicrobial agents. Immunizations targeting *G. parasuis* are employed for infection prevention and control, yet their effectiveness is confined to bacterial isolates of a particular serotype. Additionally, antibiotics are commonly used to treat the *G. parasuis* infection in veterinary clinical practice, whereas the long-term inappropriate use escalates antibiotic resistance and residue levels [37, 38]. Hence, it is urgently needed to screen the alternative drugs with anti-bacterial and anti-inflammatory properties, as well as obvious efficacy, high safety and less adverse reactions.

The regulation of QseBC TCS is crucial for the growth, metabolism, and proliferation of bacteria as it stringently regulates and controls the essential biological processes within the bacteria cells [7]. Li et al.. reported that inactivating QseBC resulted in reduced ability of biofilm formation and heightened sensitivity to antibiotics [39]. Similarly, QseC played a vital role in controlling the iron homeostasis of *G. parasuis* [9]. Therefore, QseBC TCS is a promising target to develop broad-spectrum drugs to control microbial infections. Over the past few years, multiple studies focused on the QseBC inhibitors. 2-AG antagonized the bacterial receptor QseC in enteric

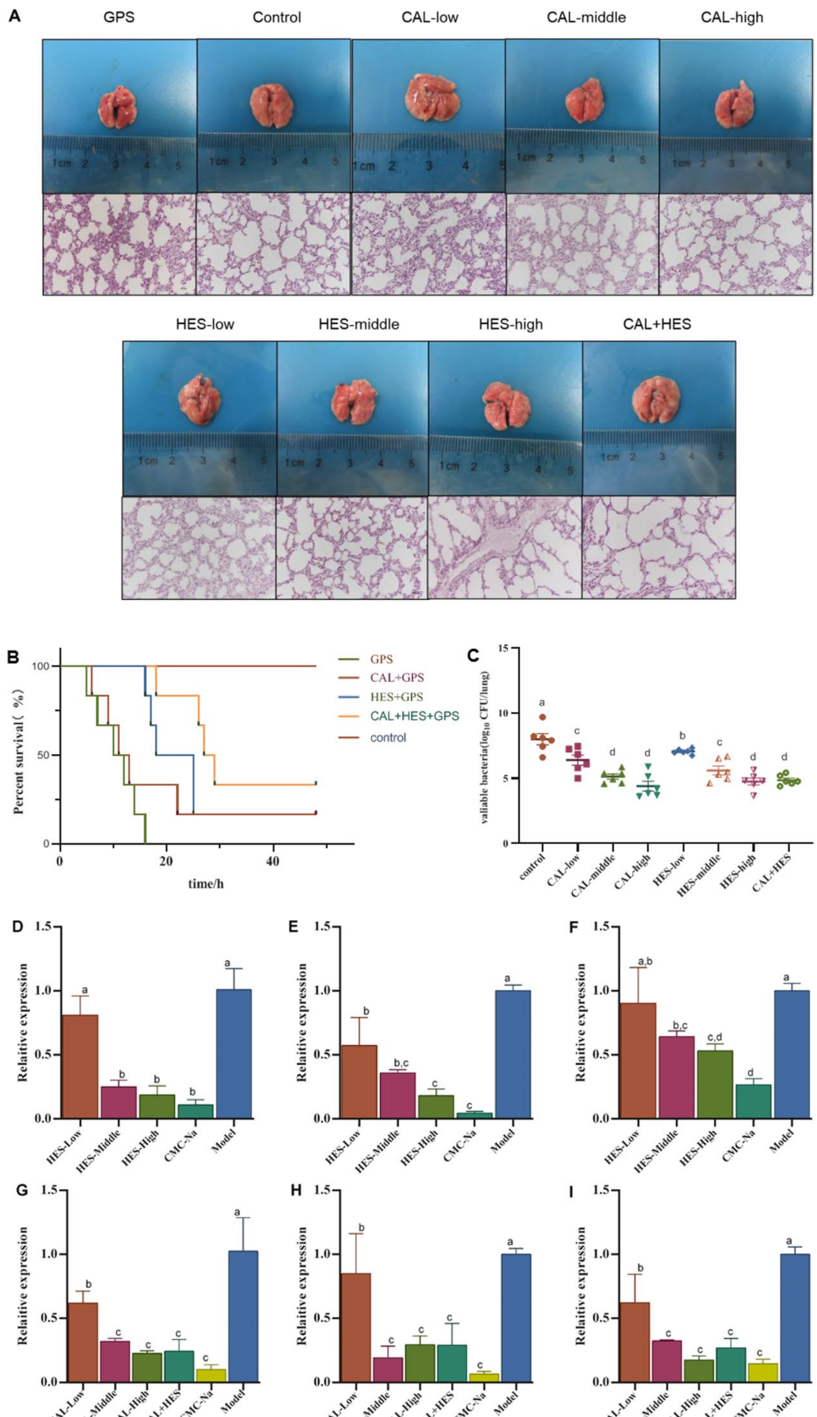

Fig. 10 The protective effect of CAL and HES on *G. parasuis* infection. **A**, Representative images of lung tissues and H&E staining of lung sections; **B**, Survival rate of mice treated with CAL and HES; **C**, The infectious bacterial load in the lung of mice treated with CAL and HES; **D-I**, The expression levels of IFN-γ, IL-6 and TNF-α in *G. parasuis* infected mice with or without CAL and HES treatment. Values denoted by varying lowercase letters signify a notable difference in every treatment ($P<0.05$), whereas those with identical lowercase letters denote no significant difference ($P>0.05$)

pathogens, which stimulated the activation of type three secretion systems linked to pathogens [40]. LED209 was regarded as prodrug with a high specificity towards QseC in *Salmonella enterica*, which was damaged in the process of in vitro and infected mice with the function of the QseC [41]. However, the QseBC inhibitors for *G. parasuis* remain limited. We sought to identify the QseBC inhibitors based on the regulatory effects of

QseBC on the biofilm formation, virulence, antibiotic resistance, flagellar-mediated bacterial motility, resistance to host immune response, iron metabolism in *G. parasuis*, and the regulation of QseBC related genes of *G. parasuis*.

CAL is a key ingredient in cinnamon essential oil with strong antimicrobial activity. Duan et al. indicated that the MICs of CAL for *E. coli*, *Pseudomonas aeruginosa* and *Staphylococcus aureus* were all 0.25 μL/mL, and 0.125 μL/mL for *Salmonella enterica* serovar Typhimurium [42].Typically, citrus bioflavonoids seem to be highly safe and devoid of adverse effects, such as HES and its glycoside forms. Choi et al. demonstrated that HES effectively inhibited the *Bacillus cereus*, *E. coli* and *P. aeruginosa* with MICs 125–500 μg/mL [19].Our results indicated that the MICs of CAL and HES were both 128 μg/mL for *G. parasuis*. Additionally, the combination of CAL or HES with AMP and AMK showed partial synergistic effect. It is noteworthy that *G parasuis* is intrinsically resistant to macrolides, while our results indicated that the combination of TAT, a macrolide antibiotic, with CAL and HES showed partial synergistic effect and synergistic effect, respectively.

As shown in Fig. 2A-C, the concentration-dependent inhibitory effect of CAL and HES on *G. parasuis* biofilm formation was evident. Additionally, the different concentrations of CAL and HES also had obvious inhibitory effect on extracellular DNA and extracellular protein during *G. parasuis* biofilm formation (Fig. 3A-F). Likewise, the results also indicated that CAL and HES showed obvious inhibitory effect on biofilm formation according to morphological changes of *G. parasuis* cells (Fig. 5). Biofilms contribute to the antibiotic resistance by several mechanisms, and it initiates when several bacterial cells adhered to a substrate. Subsequently, the bacteria release the extracellular polymeric substance (EPS), which constituted the extracellular matrix [43]. PS facilitates the breakdown of diverse substances outside the cell and increases the levels of enzymatic protections against antibiotics by hindering the dispersion of extracellular enzymes [44]. Usually, biofilms are too large for neutrophils to ingest, yet they can endure and proliferate at elevated antibiotic levels. Gradually, biofilms serve as sanctuaries for multidrug resistant plasmids, and will further promote the transfer and proliferation of multidrug resistant isolates [45, 46]. We infer that QseBC should be a potential target of antimicrobial development against *G. parasuis* as QseBC can regulate the antibiotic resistance according to a previous study [7]. Moreover, different concentrations of CAL and HES also damaged the integrity of the bacterial cell membrane (Figs. 4 and 6). He et al. found that QseBC participate in regulation of iron uptake in bacteria [9]. The proliferation of *G. parasuis* heavily relies on iron, and the host's low iron availability supply is recognized as a key pressure for the pathogenic bacteria and a signal for the major alterations in cellular activities. In this study, we found CAL and HES might inhibit the conversion of ferrous ions to ferric ions by targeting QseBC, and further reducing the virulence of *G. parasuis* (Fig. 7).

We further evaluated the expression levels of QseBC related genes via qRT-PCR (Fig. 8A-F). Among of them, β-lactam resistant related gene *oppB* (oligopeptide transporter permease) was associated with β-lactam resistance. *mraY* (Phospho-N-acetylmuramoyl-pentapeptide-transferase) is a bacterial enzyme responsible for the formation of the first lipid intermediate of the cell wall peptidoglycan synthesis, and *macB* (penicillin-binding protein lB) also plays a key role in bacterial cell wall synthesis. The cAMP receptor protein *crp* can modulate the virulence of a wide range of pathogenic bacteria, and involved in biofilm formation [47]. *cdtA* and *cdtB* are essential for the pathogenicity of *G. parasuis* as subunits of cytolethal distending toxin (CDT) [48]. Outer membrane protein P2 (*ompP2*) plays an important role in the pathogenesis of *G. parasuis* infection as a micropore protein and the most abundant protein in the outer membrane of *G. parasuis* [49]. *rbsB* (D-ribose ABC transporter substrate rate-binding protein) has a significant impact on bacterial chemotaxis, while *pilW* (type IV pilus biogenesis/stability protein) was related to bacterial flagellum. According to our results, the expressions of above genes were down-regulated at different degrees after sub-MIC concentrations of CAL and HES treatment. It is further certified that CAL and HES exerted the antimicrobial effect against *G. parasuis* by inhibiting the QseBC TCS.

Furthermore, molecular docking ranks as one of the most favored and effective in silico methods, which help forecast molecular interactions with biological entities [50]. We performed molecular docking of CAL/HES and QseBC proteins, and it is emphasized that CAL and HES produced strong interaction forces with QseBC (Fig. S1). Taken together, we supposed that CAL and HES might be inhibitors to target QseBC by inhibiting the expression of QseBC related genes, as well as interacted with proteins. Fluorescence spectroscopy has been widely used to investigate the interactions of drugs and proteins. Measuring of quenching of intrinsic fluorescence of proteins can be also applied to study binding affinity of CAL and HES to proteins. QseC, as upstream protein with histidine kinase activity, could phosphorylate the response regulator QseB, so the detection of QseC interaction with compounds can reflect the interaction of CAL/HES and TCS. We evaluated the interaction between CAL/HES and QseC protein by fluorescence quenching method [51]. CAL and HES could induce the endogenous fluorescence quenching of QseC under a mechanism of static quenching. The binding constants were detected to be 4.23×10^4 L/mol and 9.28×10^5 L/mol, and the binding site were about 2.3816 and 2.9489, respectively.

Usually, the expression of some inflammatory genes can be up-regulated after *G. parasuis* infection [38]. Our study showed that CAL and HES could effectively protect mice from *G. parasuis* infection (Fig. 10A-I). CAL and HES significantly reduced the mortality and lung bacterial load, improved lung congestion status of *G. parasuis* infected mice, and exhibited noticeable anti-inflammatory activity by down-regulating the expression of IFN-γ, IL-6 and TNF-α. Notably, the combination of low dose of CAL and HES (30 mg/kg + 30 mg/kg) has better protectiveness than the high dose of single drug, and it was in complete agreement with the results of in vitro experiment. CAL and HES are two compounds with significantly different structures, while they can both affect the QseBC. The specific mechanism needs to be more thoroughly explored in the future study. The above findings highlighted the promising therapeutic potential of CAL and HES as QseBC inhibitors for the treatment of *G. parasuis* infection. A limitation of this study was that we used the mouse model but not the swine model for preliminarily assessing the protective effect of CAL and HES against *G. parasuis*. The role and exact mechanism in swine needs to be further studied in the subsequent experiments. Another limitation of this study is that only one strain was assessed.

Conclusion

In conclusion, CAL and HES showed obvious antimicrobial activity against resistant *G. parasuis* either alone or in combination both in vitro and in vivo by several mechanisms. In vitro study indicated that CAL and HES might be QseBC inhibitors by inhibiting the expression of QseBC related genes, and interacting with the related proteins, and in vivo study indicated that CAL and HES exhibited noticeable antimicrobial and anti-inflammatory activity against *G. parasuis* infected mice. Our results highlighted the promise of CAL and HES as candidate drugs for the treatment of *G. parasuis* infection by regulating the QseBC TCS.

Abbreviations

QseBC	Quorum-sensing Escherichia coli regulators B and C
TCS	Two-component system
CAL	Cinnamaldehyde
HES	Hesperitin
AMP	Ampicillin
AMK	Amikacin
TAT	Tylvalosin
TSB	Tryptice Soy Broth
TSA	Tryptice Soy Agar
DMSO	Dimethyl sulfoxide
CLSM	Confocal laser scanning microscope
SEM	Scanning electron microscope
qRT-PCR	Quantitative reverse transcription polymerase chain reaction
FBS	Fetal bovine serum
NAD	Nicotinamide adenine dinucleotide
MIC	Minimum inhibitory concentration
CMC-Na	Carboxymethylcellulose sodium
CLSI	Clinical and Laboratory Standards Institute
FICI	Fractional inhibitory concentration index
SDS-PAGE	Sodium dodecyl sulfate polyacrylamide gel electrophoresis

Supplementary Information

The online version contains supplementary material available at https://doi.org/10.1186/s12917-025-04638-7.

Supplementary Material 1

Acknowledgements

The authors would like to acknowledge the research funds from the Agricultural Special Fund Project of Shaanxi Province (No. XNDY-202202), and Undergraduate Training Program for Innovation and Entrepreneurship of Shaanxi (No. S202310712590).

Author contributions

All authors prepared conception and design of the study. JRZ conducted laboratory analyzes, JRZ, LL, and YJG statistically analyzed the data. JRZ, YJG, and JLC performed analysis, data curation and interpretation. JRZ, LL, and YHW drafted the manuscript. JRZ, LL, WHZ, JT, YS and XQL carried out final writing, critical review and revision. XQL funded the experiment. All authors have read and approved the final manuscript.

Funding

The authors would like to acknowledge the research funds from the Agricultural Special Fund Project of Shaanxi Province (No. XNDY-202202), and Undergraduate Training Program for Innovation and Entrepreneurship of Shaanxi (No. S202310712590).

Data availability

No datasets were generated or analysed during the current study.

Declarations

Ethics approval and consent to participate

All animal experiments for this study were approved by the guidelines of the Animals Ethics Committee of Northwest A&F University (2021052).

Consent for publication

No applicable.

Competing interests

The authors declare no competing interests.

Received: 8 May 2024 / Accepted: 3 March 2025
Published online: 12 April 2025

References

1. Fu S, Yin R, Zuo S, Liu J, Zhang Y, Guo L, Qiu Y, Ye C, Liu Y, Wu Z, et al. The effects of Baicalin on piglets challenged with *Glaesserella parasuis*. Vet Res. 2020;51(1):102.
2. Gong H, Chen L, He Y, Hua K, Ma B, Gao Y, Xu X, Hu X, Jin H. Pleural thickening induced by *Glaesserella parasuis* infection was linked to increased collagen and Elastin. Front Cell Infect Microbiol. 2022;12:952377.
3. Liu F, Gao Y, Jiao J, Zhang Y, Li J, Ding L, Zhang L, Chen Z, Song X, Yang G et al. Upregulation of TLR4-dependent ATP production is critical for *Glaesserella parasuis* LPS-mediated inflammation. Cells 2023, 12(5).
4. Rivera-Benítez JF, De la Luz-Armendáriz J, Gómez-Núñez L, Vargas FD, Escatell GS, Ramírez-Medina E, Velázquez-Salinas L, Ramírez-Mendoza H, Ayala MAC, Tufiño-Loza C, et al. Swine health: history, challenges and prospects. Rev Mex Cienc Pecu. 2021;12:149–85.

5. Costa-Hurtado M, Barba-Vidal E, Maldonado J, Aragon V. Update on Glasser's disease: How to control the disease under restrictive use of antimicrobials. Vet Microbiol. 2020;242:108595.
6. Zhou T, Huang JH, Liu ZQ, Lin QQ, Xu ZL, Zhang LH. The Two-component system FleS/FleR represses H1-T6SS via Cyclic di-GMP signaling in *Pseudomonas aeruginosa*. Appl Environ Microb 2022, 88(2).
7. Zhu YX, Dou Q, Du LC, Wang Y. QseB/QseC: a two-component system globally regulating bacterial behaviors. Trends Microbiol. 2023;31(7):749–62.
8. Hughes DT, Clarke MB, Yamamoto K, Rasko DA, Sperandio V. The QseC adrenergic signaling cascade in enterohemorrhagic *Escherichia coli* (EHEC). Plos Pathog 2009, 5(8).
9. He LQ, Dai K, Wen XT, Ding LQ, Cao SJ, Huang XB, Wu R, Zhao Q, Huang Y, Yan QG et al. QseC mediates osmotic stress resistance and biofilm formation in *Haemophilus parasuis*. Front Microbiol. 2018;9:212.
10. Darakhshan S, Bidmeshki Pour A, Hosseinzadeh Colagar A, Sisakhtnezhad S. Thymoquinone and its therapeutic potentials. Pharmacol Res. 2015;95–96:138–58.
11. Yin L, Dai Y, Chen H, He X, Ouyang P, Huang X, Sun X, Ai Y, Lai S, Zhu L et al. Cinnamaldehyde resist Salmonella Typhimurium adhesion by inhibiting type I fimbriae. Molecules 2022, 27(22).
12. He ZY, Huang ZW, Jiang W, Zhou W. Antimicrobial activity of cinnamaldehyde on *Streptococcus mutants* biofilms. Front Microbiol. 2019;10:2241.
13. Utchariyakiat I, Surassmo S, Jaturanpinyo M, Khuntayaporn P, Chomnawang MT. Efficacy of cinnamon bark oil and cinnamaldehyde on anti-multidrug resistant *Pseudomonas aeruginosa* and the synergistic effects in combination with other antimicrobial agents. BMC Complem Altern M. 2016;16:158.
14. Wang R, Li S, Jia H, Si X, Lei Y, Lyu J, Dai Z, Wu Z. Protective effects of cinnamaldehyde on the inflammatory response, oxidative stress, and apoptosis in liver of Salmonella typhimurium-challenged mice. Molecules 2021, 26(8).
15. Yu HH, Song YJ, Yu HS, Lee NK, Paik HD. Investigating the antimicrobial and antibiofilm effects of cinnamaldehyde against *Campylobacte* spp. Using cell surface characteristics. J Food Sci. 2020;85(1):157–64.
16. Barbosa PDM, Ruviaro AR, Martins IM, Macedo JA, LaPointe G, Macedo GA. Enzyme-assisted extraction of flavanones from citrus pomace: obtention of natural compounds with anti-virulence and anti-adhesive effect against *Salmonella enterica* subsp. enterica serovar typhimurium. Food Control. 2021;120:107525.
17. Yao K, Mu QC, Zhang YF, Cheng Q, Cheng XZ, Liu XJ, Luo CM, Li CM, Cai SX, Luo ZC et al. Hesperetin nanoparticle targeting neutrophils for enhanced TBI therapy. *Adv Funct Mater* 2022, 32(43).
18. Yuan F, Xia GQ, Cai JN, Lv XW, Dai M. Hesperitin attenuates alcoholic steatohepatitis by regulating TLR4/NF-κB signaling in mice. Anal Biochem. 2023;682:115339.
19. Choi SS, Lee SH, Lee KA. A comparative study of Hesperetin, hesperidin and hesperidin glucoside: antioxidant, anti-inflammatory, and antibacterial activities *in vitro*. Antioxidants-Basel 2022, 11(8).
20. Zhao SQ, Nan YZ, Yao RY, Wang LH, Zeng XA, Aadil RM, Shabbir MA. Antibacterial activity and transcriptomic analysis of Hesperetin against *Alicyclobacillus acidoterrestris* vegetative cells. Foods 2023, 12(17).
21. Clinical and Laboratory Standards Institute (CLSI). Performance standards for antimicrobial susceptibility testing; Thirty informational supplement, CLSI document M100-S30. Clinical and laboratory standards Institute. Wayne PA; 2020.
22. Prüller S, Turni C, Blackall PJ, Beyerbach M, Klein G, Kreienbrock L, Strutzberg-Minder K, Kaspar H, Meemken D, Kehrenberg C. Towards a standardized method for broth microdilution susceptibility testing of *Haemophilus parasuis*. J Clin Microbiol. 2017;55(1):264–73.
23. Zhou Y-F, Bu M-X, Liu P, Sun J, Liu Y-H, Liao X-P. Epidemiological and PK/PD cutoff values determination and PK/PD-based dose assessment of Gamithromycin against *Haemophilus parasuis* in piglets. BMC Vet Res. 2020;16(1):81.
24. Lei ZX, Fu SL, Yang B, Liu QY, Ahmed S, Xu L, Xiong JC, Cao JY, Qiu YS. Comparative transcriptional profiling of tildipirosin-resistant and sensitive. Sci Rep-UK. 2017;7:7517.
25. Xu ZH, Huang AX, Luo X, Zhang P, Huang LL, Wang X, Mi K, Fang SW, Huang X, Li J et al. Exploration of clinical breakpoint of Danofloxacin for *Glaesserella parasuis* in plasma and in PELF. Antibiotics-Basel 2021, 10(7).
26. Tong YC, Li PC, Yang Y, Lin QY, Liu JT, Gao YN, Zhang YN, Jin S, Qing SZ, Xing FS et al. Detection of antibiotic resistance in feline-origin ESBL *Escherichia coli* from different areas of China and the resistance elimination of Garlic oil to cefquinome on ESBL *E. coli*. Int J Mol Sci 2023, 24(11).
27. Vazquez-Armenta FJ, Bernal-Mercado AT, Tapia-Rodriguez MR, Gonzalez-Aguilar GA, Lopez-Zavala AA, Martinez-Tellez MA, Hernandez-Oñate MA, Ayala-Zavala JF. Quercetin reduces adhesion and inhibits biofilm development by *Listeria monocytogenes* by reducing the amount of extracellular proteins. Food Control. 2018;90:266–73.
28. Han RJ, Xing JB, Sun HR, Guo ZY, Yi KF, Hu GZ, Zhai YJ, Velkov T, Wu H. The antihelminth drug rafoxanide reverses chromosomal-mediated colistin-resistance in. *mSphere* 2023.
29. Zhou WR, Mao BY, Tang X, Zhang QX, Zhao JX, Chen W, Cui SM. Cyclopropane fatty acid and accumulation of glutamate contributed to higher freeze-drying resistance for Bifidobacterium animalis than Bifidobacterium adolescentis. Food Biosci. 2023;56:103353.
30. Yu SM, Peng YP, Yu SJ, Lü H, Guo C. Interaction between latex microspheres and antibody proteins revealed by fluorescence spectroscopy. Spectrosc Spect Anal. 2012;32(8):2166–70.
31. Jiang RJ, Xiang MY, Chen WT, Zhang PF, Wu XL, Zhu GH, Tu T, Jiang DK, Yao XP, Luo Y et al. Biofilm characteristics and transcriptomic analysis of Haemophilus parasuis. Vet Microbiol. 2021;258:109073.
32. Dong HB, Yu P, Long B, Peng T, He YJ, Xu B, Liao L, Lu L. Total synthesis of Kuwanons A and B and discovery of their antibacterial mechanism. J Nat Prod. 2023;86(8):2022–30.
33. Zhong ZX, Zhou S, Liang YJ, Wei YY, Li Y, Long TF, He Q, Li MY, Zhou YF, Yu Y et al. Natural flavonoids disrupt bacterial iron homeostasis to potentiate colistin efficacy. Sci Adv. 2023;9(23).
34. Liu MX, Wang Q, Wu WD, Chen M, Zhang PY, Guo MR, Lin HX, Ma Z, Zhou H, Fan HJ. *Glaesserella parasuis* serotype 5 breaches the Porcine respiratory epithelial barrier by inducing autophagy and blocking the cell membrane Claudin-1 replenishment. Plos Pathog 2022, 18(10).
35. Brogden S, Pavlovic A, Tegeler R, Kaspar H, De Vaan N, Kehrenberg C. Antimicrobial susceptibility of *Haemophilus Parasui* isolates from Germany by use of a proposed standard method for harmonized testing. Vet Microbiol. 2018;217:32–5.
36. Huang AX, Huang X, Zhang ZH, Yuan ZH, Huang LL, Wang YL, Tao YF, Chen DM, Liu ZL, Hao HH. Dosing regimen of aditoprim and sulfamethoxazole combination for the *Glaesserella parasuis* containing resistance and virulence genes. Pharmaceutics 2022, 14(10).
37. He CL, Yang PY, Wang L, Jiang XL, Zhang W, Liang XX, Yin LZ, Yin ZQ, Geng Y, Zhong ZJ, et al. Antibacterial effect of *Blumea balsamifera* (L.) DC. essential oil against *Staphylococcusaureus*. Arch Microbiol. 2020;202(9):2499–508.
38. Ye C, Li RZ, Xu L, Qiu YS, Fu SL, Liu Y, Wu ZY, Hou YQ, Hu CAA. Effects of Baicalin on piglet monocytes involving PKC-MAPK signaling pathways induced by *Haemophilus parasuis*. BMC Vet Res. 2019;15:98.
39. Li WC, Xue M, Yu LM, Qi KZ, Ni JT, Chen XL, Deng RN, Shang F, Xue T. QseBC is involved in the biofilm formation and antibiotic resistance in *Escherichia coli* isolated from bovine mastitis. PeerJ. 2020;8:e8833.
40. Ellermann M, Pacheco AR, Jimenez AG, Russell RM, Cuesta S, Kumar A, Zhu WH, Vale G, Martin SA, Raj P, et al. Endocannabinoids inhibit the induction of virulence in enteric pathogens. Cell. 2020;183(3):650–.
41. Curtis MM, Russell R, Moreira CG, Adebesin AM, Wang CG, Williams NS, Taussig R, Stewart D, Zimmern P, Lu BA et al. QseC inhibitors as an antivirulence approach for gram-negative pathogens. Mbio 2014, 5(6).
42. Duan XJ, Qin DY, Li HM, Zhang T, Han YL, Huang YQ, He D, Wu KG, Chai XH, Chen C. Study of antimicrobial activity and mechanism of vapor-phase cinnamaldehyde for killing *Escherichia coli* based on fumigation method. Front Nutr. 2022;9:1040152.
43. Trubenová B, Roizman D, Moter A, Rolff J, Regoes RR. Population genetics,biofilm recalcitrance, and antibiotic resistance evolution. Trends Microbiol. 2022;30(9):841–52.
44. Wang LF, Li Y, Wang L, Zhu MJ, Zhu XX, Qian C, Li WW. Responses of biofilm microorganisms from moving bed biofilm reactor to antibiotics exposure: protective role of extracellular polymeric substances. Bioresource Technol. 2018;254:268–77.
45. Yan J, Bassler BL. Surviving as a community: antibiotic tolerance and persistence in bacterial biofilms. Cell Host Microbe. 2019;26(1):15–21.
46. Metzger GA, Ridenhour BJ, France M, Gliniewicz K, Millstein J, Settles ML, Forney LJ, Stalder T, Top EM. Biofilms preserve the transmissibility of a multi-drug resistance plasmid. Npj Biofilms Microbi 2022, 8(1).
47. Jiang CS, Ren JP, Zhang XQ, Li C, Hu YF, Cao H, Zeng W, Li ZH, He QG. Deletion of the *crp* gene affects the virulence and the activation of the NF-κB and MAPK signaling pathways in PK-15 and iPAM cells derived from *G. parasuis* serovar 5. *Veterinary microbiology* 2021, 261.
48. Chen QC, Wang H, Li L, Guo SB, Liu ZK, Hu ZZ, Tan C, Chen HC, Wang XR. Characterization of a universal neutralizing monoclonal antibody against *Glaesserella parasuis* CdtB. Vet Microbiol. 2022;270:109446.

49. Zhou SM, He XH, Xu CG, Zhang B, Feng SX, Zou Y, Li JY, Liao M. The outer membrane protein P2 (*OmpP2*) of *Haemophilus Parasui* induces Proinflammatory cytokine mRNA expression in Porcine alveolar macrophages. Vet J. 2014;199(3):461–4.
50. Pinzi L, Rastelli G. Molecular docking: shifting paradigms in drug discovery. Int J Mol Sci 2019, 20(18).
51. Du J, Xia ZN. Interactions of gold nanoparticles and lysozyme by fluorescence quenching method. Anal Lett. 2012;45(15):2236–45.

Publisher's note